Article:
Gadi, VK, Bordoloi, S, Garg, A et al. (2018) Effect of shoot parameters on cracking in vegetated soil. Environmental Geotechnics, 5 (2). pp. 123-130. ISSN: 2051-803X

https://doi.org/10.1680/jenge.17.00013

Effect of shoot parameters on cracking in vegetated soil

Vinay Kumar Gadi, Sanandam Bordoloi, *Ankit Garg, Lingaraj Sahoo, Christian Berretta and Sreedeep Sekharan

Name: Vinay Kumar Gadi
Affiliation: B.Tech, M.Tech
Title: Research student
Address: Department of Civil Engineering, Indian Institute of Technology Guwahati, India
E-mail: vinay.gadi@iitg.ernet.in, **Telephone**: +91-9440381364

Name: Sanandam Bordoloi
Affiliation: B.E, M.E
Title: Research student
Address: Department of Civil Engineering, Indian Institute of Technology Guwahati, India
E-mail: sanandam@iitg.ernet.in, **Telephone**: +91-9706381570

Name: Dr Ankit Garg* (Corresponding author)
Affiliation: B.Tech, PhD
Title: Associate Professor
Address: Department of Civil and Environmental Engineering, Shantou University, China
E-mail: ankit@stu.edu.cn, **Telephone**: +86-15007542863

Name: Dr Lingaraj Sahoo
Affiliation: BSc, MSc, PhD
Title: Professor
Address: Department of Biosciences and Bioengineering Engineering, Indian Institute of Technology Guwahati, India.
E-mail: ls@iitg.ernet.in, **Telephone**: +91-9957467836

Name: Dr Christian Berretta
Affiliation: BEng, MSc, PhD
Title: Academic Research Fellow
Address: School of Civil Engineering, University of Leeds, Leeds, LS2 9JT, UK
E-mail: C.Berretta@leeds.ac.uk, **Telephone**: +44 (0)113 3432248

Name: Dr Sreedeep Sekharan
Affiliation: B.Tech, M.Tech, PhD
Title: Professor
Address: Department of Civil Engineering, Indian Institute of Technology Guwahati, India
E-mail: srees@iitgernet.in, **Telephone**: +91-9957183636

Abstract

The relationship of shoot parameters, which play a major role in transpiration, with the cracking of soil has rarely been investigated. Such relation helps to analyse water use efficiency accurately. This study investigated the effect of vegetation (cowpea) age on crack formation and explored any correlation between age and cracking. The age of vegetation was expressed in the form of shoot parameters (shoot length (SL) and leaf area index (LAI)). Crack formation was expressed in the form of crack intensity factor (CIF). Ten experimental test pots were used to observe crack formation on vegetated and bare soil in a greenhouse. Image analysis in the experimental pots revealed that under drying–wetting cycles, the CIF of vegetated soil increased compared with that of bare soil. There was an evident increase in CIF with SL growth, up to a threshold length (400 mm), where lateral branch growth starts forming. There was no observable increase in CIF, with further SL growth (with negligible lateral branch formation). CIF increased with LAI up to a certain threshold value (0·56), after which the CIF was relatively the same. Two correlations have been identified for shoot parameters (SL, LAI) with the CIF for the selected species.

Keywords: Drying-wetting cycle, Crack formation, SL, LAI, CIF, cowpea

1. Introduction

Desiccation cracking is a common phenomenon in fine grained soil, and is observed in undisturbed soil on drying. A desiccation crack occurs when the drying induced surface tensile stress (suction) reaches the soil tensile strength (Corte and Higashi, 1960). These cracks on the surface expose the interior of the soil to climatic conditions (Yesiller et al., 2000). Cracks in soil have implication in agriculture engineering (Torres et al., 2004; Gadi et al. 2016), landfill clay liner system (Costa et al., 2013), road embankments (Gadi et al., 2016) and green infrastructure (Stovin et al., 2013; Berretta et al., 2014; Bordoloi et al. 2015; Bordoloi et al., 2016; Vardhan et al., 2017; Bordoloi et al., 2017a;b;c;d). Surface cracking has both positive and negative attributes in the field of agriculture. Improved drainage during harvest of crop (Bouma et al., 1979; Yoshida and Adachi, 2003), improved infiltration (Swartz, 1966) and solute-microorganism transport (Ringrose-Voase and Sanidad, 1996; Chertkov and Ravina, 1999) are such positive attributes of desiccation cracks in agricultural field. However, rapid transport of water and solute through soil cracks, leads to drought condition (Thomas and Phillips, 1979) and nutrient leaching (Coles and Trudgill, 1985) respectively. Moreover, such cracks are the precursor for the formation of gullies, which ultimately leads to fertile soil loss due to erosion (Ollobarren et al., 2016). Cracks also facilitate excess soil water evaporation in agricultural fields by opening up secondary evaporation planes in its profile (Torres et al., 2004).

The effect of cracking on landfill clay liners has garnered considerable attention in the recent past. Clay liners are susceptible to cracking during cycles of drying-wetting, which eventually is detrimental to the integrity of the liner (Andersland and Al-Moussawi, 1987; Albright et al., 2006; Li and Zhang, 2010; Costa et al., 2013). Surface cracks can have marked increase of water infiltration into the liner material and subsequently give rise to excess leachate generation

(Snow, 1969; Yuen et al., 1998; Rayhani et al., 2008; Li et al., 2011; Bordoloi et al. 2017). The liner cover material is mostly covered with vegetation (Waugh et al., 1994), to minimize soil erosion. The crack formation and intensity are influenced by the plant cover distribution (Johnston and Hill, 1944; Dasog et al., 1988) and type of crop (Fox, 1964, Mitchell and van Genuchten, 1992). Upon vegetation induced transpiration, soil moisture would be further reduced through root-water uptake, as compared to bare soil (Blight, 2003; Hemmati et al., 2012). Thus vegetation leads to transpiration induced suction in the soil. Li et al. (2016) recently have studied the effect of *Festuca arundinacea* grass on cracking on liner material. However, they have not considered the effect of shoot parameters on crack formation in the soil. Shoot parameters (LAI, SL) greatly affect transpiration induced suction, because of their influence on intercepted radiant energy (Leung et al., 2015a, b; Garg et al. 2015b; Gadi et al., 2017; Hazra et al. 2017)). LAI is defined as the one-sided green leaf area per unit ground canopy area. As far as authors are aware, rarely any studies have been done to correlate such shoot parameters with quantitative crack parameter for repeated drying-wetting cycles as commonly encountered due to seasonal effect and irrigation.

Quantification of crack in soil is important to model water retention, flow and balance at surface (Arnold et al. 2005, Baer et al. 2009) of any topography. Basic measurement of cracks has been reported in past studies. Manual measurement using a bilateral device consisting of a wire probe to measure crack width has been devised (El Abedine and Robinson, 1971). Soil crack distribution in situ has been measured using polythene sheets by Logsdon et al. (1990). Such conventional manual measurement techniques are difficult to measure the highly irregular crack network (Tang et al., 2012). Hence, digital image-processing approaches are attaining increased acceptance in the field of soil characterization due to its non-destructive analysis and accuracy (Macai et al., 1993; Anand et al., 2004). The widely accepted CIF approach using captured images

(Yesiller et al., 2000; Li et al., 2016) has been used extensively to measure and quantify cracks. The CIF approach has been used in many studies (Mi, 1995; Miller et al., 1998; Yesiller et al., 2000; Li et al., 2016; Chaduvula et al. 2017; Wang et al. 2017; Jayanthi et al. 2017) as a descriptor of the extent of surficial cracking.

The main objective of the current work is to study the effect of vegetation age on cracking for a plant species, *cowpea.* Age of vegetation was expressed in form of shoot parameters (SL and LAI). Crack formation was expressed in form of CIF. The study explores correlations between shoot parameters (SL and LAI) and CIF for the species. Such correlations will be helpful to design proper drainage schemes in any terrain, analyze water use efficiency and model water balance accurately for vegetated field.

2. Material and methods

2.1 Soil property

The soil is classified as ML, according to unified soil classification system (USCS) (ASTM D2487-11). Grain size distribution of the soil reveal that the soil constituted mainly of silt (50 %) and clay (25 %), followed by fine sand (19%) and medium sand (6 %). Liquid limit, plastic limit and shrinkage limit are 41 %, 25 % and 13 % respectively. Basic physical and engineering properties are summarized in **Table .1**. The determination of these properties has been determined under the provisions of ASTM codes (ASTM D854-06; ASTM D2487-10; ASTM D698-07 and ASTM D4318-93).

2.2 Selected plant species and germination condition

The vegetation type selected is a crop species, Cowpea (*Vigna unguiculata*). Cowpea is an important crop widely cultivated by farmers in Sub Saharan countries and Asia, Africa and America (Singh et al., 2003). Cowpea is well known for its adaptation to nutrient poor soils (Solleti et al., 2008). The growth stage of cowpea is generally classified into three stages, namely vegetative growth stage (30-40 days), reproductive growth stage (20 days) and physiological maturity stage (15 days) (Mass and Poss 1988, Agyeman et al. 2014). However, the maturity time (63 -80 days) is reported to vary due to different local climatic conditions and species (Agyeman et al. 2014). The mature seeds of cowpea cultivar, Pusa Komal were procured from Seed Corporation of India, New Delhi. The seeds were germinated on cotton moistened with tap water, in petri dishes for three days in dark, at 25 ^{0}C under florescent light (140 µE $m^{-2}s^{-1}$). The germinated seedlings were transferred to the pots for conducting experiments.

2.3 Test plan

A test plan is designed to quantify and compare CIF between bare and vegetated soil in controlled irrigation for a period of 70 days until the plant completes reproductive growth stage. Apart from irrigation, plant parameters were subjected to natural environmental conditions. All the experiments were conducted in a greenhouse (**Fig. 1**). In total, 10 pots (5 vegetated pots, 5 bare pots) were monitored in the test duration. The seedlings of the plant species were germinated and transplanted to the 5 pots. All the 10 pots were irrigated at a regular interval. The evaporation/evapotranspiration rate was measured regularly and reported in later section. The SL was measured manually and the crack surface and LAI were measured using image analysis as discussed in a later section.

2.4 Experimental setup

The relative humidity and temperature were observed at 52 ±8 % and 26 ±4 ^{0}C, respectively. To provide radiant energy to the legume seedlings, a provision of white fluorescent lamps capable of emitting light with photosynthetic photon flux density of 50 μmol m^{-2} s^{-1} was mounted on top (2.5 m from floor base). The cylindrical pots used to conduct experiment were made from PVC plastic in house. Its dimensions are 260 mm diameter and 230 mm depth with perforated base to allow water drainage from the bottom. The soil was compacted in three equal layers to maintain a uniform density of 1.3 g/cc (equivalent to 0.77 maximum dry density of soil) up to 185 mm from bottom. All the 10 pots were irrigated (400 mL per pot using a watering can) regularly after 3 days of interval as shown in **Fig. 2** after transplantation. Evapotranspiration and evaporation rate of the 5 vegetated and 5 bare pots respectively was measured by observing change in weight. **Fig. 2** shows the mean and standard deviation of evaporation/evapotranspiration rate after transplantation (3 day interval). The weight change of vegetated soil pot over a drying cycle was measured using weighing balance. The measured change in weight indicates the loss of water i.e., evapotranspiration. Similar to this, change in weight of bare soil over a drying cycle due to loss of water was reported as evaporation. It is to be noted that the evapotranspiration and evaporation rate noted in the study has been calculated for all 10 different pots individually. SL for all the vegetated pots has been measured using a metric scale at the same 3 day interval after transplantation. The surface crack formation and leaf area photos have been captured regularly after 9 days interval starting from 15th day after transplantation, using image analysis as discussed in the following section. Canon EOS 600D with lens range (18-55 mm), horizontal/vertical resolution of 72 dpi was used to capture images under early morning ambient light. The exposure time, focal length and ISO speed was maintained at 1/30 sec, 23 mm and ISO-640 respectively for crack analysis. Photographs were captured carefully from the same angle (45^0) and height (0.75m from floor base) using a frame with adjustable height (**Fig. 3**), to minimize any observational error for CIF analysis. In case of LAI analysis, the exposure time, focal length and ISO speed was maintained at 1/60 sec, 30 mm and ISO-400 respectively. The photographs for LAI were captured from a fixed position (1.5m above and parallel to the floor base). It is to be noted that the photographic conditions was maintained for all tested pots and the pictures were taken at early morning conditions.

2.5 Procedure for analysis of CIF and LAI

In this study, the image-processing software ImageJ (Rasband, 2012), has been used to analyze the surface crack and leaf area. The surface crack has been analyzed using the CIF parameter which is the ratio of crack area (A_c) to the total area of soil considered (A_t). The 'A_c' and 'A_t' of drying soil mass were determined using photographs of desiccating soil after regular interval of time (15, 24, 33, 42, 51, 60 and 69 days; at various ages of plants) from transplantation. Cracks appear darker than remaining uncracked soil in photographs of a drying soil (Yesiller et al., 2000). This color contrast between cracked and uncracked soil for the same photographic condition is used to analyze CIF. For CIF analysis, the captured image is imported into ImageJ, and the digitized image is cropped to only account for the soil surface as shown in **Fig. 3**. The image was cropped such that any boundary shrinkage was excluded and only surface cracks were taken for further analysis.

In order to calculate the areas, the cropped image was transformed into binary image as shown in **Fig. 3.** The pixels that are occupied by the cracks (white portion) and by the total soil surface (both white and black) is calculated to obtain CIF of soil. To ensure equal soil surface area analyzed for all pots, each pot was calibrated to account for equal number of pixel area. This was done by maintaining same height and angle of captured image and it was cross checked by observing the pixel area (accuracy of ±2%) for the soil pot. For example in **Fig. 3**, 560 cm^2 soil area of pot (dia = 26 cm) was calibrated to 7719028 pixels.

The LAI of the vegetated soil is obtained using color threshold technique using ImageJ. As in the case of CIF calculation, the captured image is imported into ImageJ, and the digitized image is cropped to only account for the plant canopy as shown in **Fig. 3**. To calculate the leaf area, the cropped image was adjusted (for hue, saturation and brightness) using (Threshold Color) option in the software (refer **Fig. 3**). Under this option, only those pixels are selected that fall under the leaf color (white portion in **Fig. 3**). These pixels are calculated and taken into account as leaf area. The ratio of the leaf area and total plant canopy area is used to calculate LAI. Any noise (unwanted area) was subtracted in both measurements (CIF and LAI).

3. Result and discussion

3.1 Variation of crack intensity factor with time for both bare and vegetated soil

As shown in **Fig. 4(a)**, the mean CIF value for bare soil increased almost from 0.93 to 3.22 up to 51 days. From 51 to 70 days, the CIF value is seen to be relatively constant. This trend has been observed in previous literature (Tang et al., 2012; Li et al., 2016; Wang et al. 2017). The CIF variation for bare soil has been fitted and represented in Equation 1. The R^2 value of Equation 1 is

0.97. The analyzed time-lapse binary image of cracked soil for a particular bare pot has been shown in **Fig. 4(b)**.

$$CIF_{bare} = -0.0004t^2 + 0.0772t + 0.1752 \qquad \text{(where } 15 \leq t \text{ (days)} \leq 70\text{)} \quad \text{---- (1)}$$

This increase in CIF can be attributed to repeating drying-wetting cycles as reported in similar studies with clay (Yesiller et al., 2000; Tang et al., 2012; Li et al., 2016; Wang et al. 2017). During the drying cycle, the soil possesses relatively high soil strength which resists cracking (tensile) forces related to high suction. The drying spell is accompanied by shrinkage of soil which further causes structural rearrangement of soil particles and potential breaking of bonds (Yong and Warkentin, 1975). The subsequent wetting cycle causes decrease in soil strength. This in turn, increases tendency of cracking in next drying cycle (Yesiller et al., 2000).

On the other hand, for vegetated soil, a similar trend has been observed in variation of CIF for the first 33 days in all 3 vegetated pots. The mean CIF increase from 0.93 to 5 for the initial 33 days and the CIF remained relatively constant thereafter up to 70 days. The CIF values for vegetated soil were observed to be greater than bare soil as shown in **Fig. 4(a)**. This relative increase of CIF values for vegetated soil can be attributed to transpiration induced suction. As observed in **Fig. 2**, the evapotranspiration rate of vegetated soil is much higher than the evaporation rate of bare soil. This results in relatively higher suction (transpiration induced) in vegetated soil and correspondingly induces more cracks as compared to bare soil (Garg et al., 2015a, b, c; Leung et al., 2015b). The CIF variation for vegetated soil has been fitted into a logarithmic equation and represented in Equation 2. The R^2 value of Equation 2 is 0.97.

$$CIF_{veg} = -0.0047\, t^2 + 0.423\, t - 4.56 \qquad \text{(where } 15 \leq t \text{ (days)} \leq 70\text{)} \qquad \text{---- (2)}$$

The time lapse crack variation for the test period in a single vegetated pot has been shown in **Fig. 4(b).** The binary image representation of cracks in the pot shows that there has been an increase in cracks till 33 days after transplantation. Thereafter the crack portions are relatively same. This is due to CIF attaining its maximum potential earlier than that of bare soil due to transpiration after which there is no further increase in crack surface.

3.2 Relationship between shoot parameters and CIF for vegetated soil

The SL variation throughout the experiment span has been monitored for all the five vegetated pots up to 70 days. A linear increase in mean SL has been observed initially up to 50 days at the vegetative stage of the plant as shown in **Fig. 4**. After 50 days commencing the reproductive growth stage which is marked by flower budding, the SL growth rate decreases. This slowing down of SL is due to energy of the plant being expended for flower growth. This has been fitted as a second degree polynomial equation in Equation 3. The R^2 value of the equation is 0.99.

$$SL = -0.1287t^2 + 23.012t - 188.85 \qquad \text{(where } 9 \leq t \text{ (days)} \leq 70) \qquad \text{---- (3)}$$

The effect of SL on crack formation is proportional up to 33 days. With increase in SL there is a visible increase in CIF as shown in **Fig. 4**. This is due to increase in transpiration due to plant growth throughout this period. This period of plant growth is marked by preliminary growth of lateral branches (with leaves), which take part in enhanced transpiration. After 33 days of shoot growth (i.e. SL = 400 mm), the CIF values showed no visible increase but remain constant thereafter. The relationship between SL and CIF for the plant species has been fitted to give a three degree polynomial equation and represented in Equation 4. The R^2 value in Equation 4 is 0.97.

$$CIF_{veg} = 2E\text{-}08SL^3 - 5E\text{-}05SL^2 + 0.034SL - 2.79 \quad \text{(where } 127 \leq SL \text{ (mm) } \leq 762\text{)} \quad \text{---- (4)}$$

The LAI variation for the entire testing period has been measured using color threshold analysis using ImageJ. As shown in **Fig. 5(a)**, LAI increased from 0.24 to 0.96 with increase in time. This LAI variation with time has been fitted in Equation 5. The R^2 value is 0.99 for Equation 5.

$$LAI = -0.0002t^2 + 0.0291t - 0.1601 \qquad \text{(where } 15 \leq t \text{ (days) } \leq 70\text{)} \qquad \text{---- (5)}$$

As in the case of SL, the effect of LAI on crack formation is proportional up to 33 days after which the CIF remains relatively constant. The LAI corresponding to 33 days after transplantation was 0.56. The relationship with LAI and CIF for the entire testing period has been fitted in a two degree polynomial equation as shown in equation 6. The R^2 value of equation 6 is 0.96.

$$CIF_{veg} = -11.75\ LAI^2 + 20.15\ LAI - 3.29 \quad \text{(where } 0.24 \leq LAI \leq 0.96\text{)} \qquad \text{---- (6)}$$

In this study, LAI values are found to be low for the cow pea plants (less than 1). However, grass species may exhibit relatively higher LAI values (Garg et al., 2015b) and the equation may not be valid for such species with higher LAI. Further studies are needed for other type of species with higher LAI. The LAI variation for a single pot has been shown in **Fig. 5(b)**. It is evident that there is a gradual increase in LAI with time.

4. Summary and conclusion

The present study investigates the effect of a plant species (*cowpea)* age, on the cracking of soil for repeated drying-wetting cycles. The tests were done to explore any correlations between shoot parameters and its corresponding CIF. Based on the results and discussion, the following conclusions have been drawn and discussed.

1) Mean CIF value for bare soil increased initially from 0.93 to 3.22 at 51 days of monitoring for repeated drying-wetting cycles after which it remained relatively constant till 70 days. The mean CIF value for vegetated soil increased linearly for the first 33 days, after which there was no considerable increase in cracking. The CIF values for vegetated soil were relatively higher than bare soil throughout the test period. This increase in crack is attributed due to transpiration induced suction in case of vegetated soil.
2) The SL variation increases linearly with time after transplantation for the vegetative growth period after which the growth is relatively stunted. CIF increases linearly with SL up to a threshold value of 400 mm, marked by initiation of leaf growth in lateral branches. After attaining SL equal to 400 mm, there was no visible increase in CIF corresponding to further aging of plants. A correlation (Equation 4) has been given relating CIF_{veg} with its corresponding SL (where $127 \leq SL\ (mm) \leq 762$).
3) The LAI variation of the plant species increases with time after transplantation. The CIF_{veg} increases with LAI for the plant species up to LAI equaling 0.56. The CIF value remained relatively constant thereafter with further increase in LAI. Their correlation has been fitted as shown in Equation 6.

The obtained correlations can be adopted while designing drainage, analyzing water use efficiency and modeling water balance at surface for soil vegetated with cowpea. Further studies are required on different species to explore the threshold value of SL and LAI for other plant species. Shoot parameters such as shoot architecture, LAI (with LAI>1) needs to be incorporated in analyzing its effect on cracking for different species. Generally, shoot parameters and its corresponding CIF for heterogeneous vegetated soils maybe due to existence of multiple plants (as found in nature) and may be not be similar to those found in case of the studied species. Mutual shading, growth competition (i.e., plant-plant interaction) attributes such dissimilarity (Gadi et al. 2017). Extensive investigations need to be undertaken to measure CIF taking into account plant-plant interaction, to provide CIF correlations for a heterogeneous vegetated soil.

Acknowledgement

The authors would like to acknowledge the help provided by Shubhankar Jha, B.Tech. student for his help in conducting the experiments. The authors would like to thank Shantou University Scientific Research Fund (NTF17007) for their support.

References

A.S.T.M., D2487-10, (2010). Standard Practice for Classification of Soils for Engineering Purposes (Unified Soil Classification System). *Annual Book of ASTM Standards*.

A.S.T.M., D2487-11, (2011). Standard Practice for Classification of Soils for Engineering Purpose (Unified Soil Classification System). *Annual book of ASTM standards.*

A.S.T.M., D4318-93, (1993). Standard Test Methods for Liquid Limit, Plastic Limit and Plasticity Index of Soils. *Annual Book of ASTM Standards*.

A.S.T.M., D698-07, (2007). Standard Test Methods for Laboratory Compaction Characteristics of Soil Using Standard Effort. *Annual Book of ASTM Standards*.

A.S.T.M., D854-06, (2007). Standard test method for specific gravity of soil solids by water pycnometer. *Annual book of ASTM standards*.

Albright, W.H., Benson, C.H., Gee, G.W., Abichou, T., McDonald, E.V., Tyler, S.W. and Rock, S.A., (2006). Field performance of a compacted clay landfill final cover at a humid site. *Journal of Geotechnical and Geoenvironmental Engineering* **132(11):** pp.1393-1403.

Anand, J.P., Balakrishna, K. and Laureano, R.H., (2004). Volumetric shrinkage strain measurements in expansive soils using digital imaging technology.

Andersland, O.B. and Al-Moussawi, H.M., (1987). Crack formation in soil landfill covers due to thermal contraction. *Waste Management & Research* **5(1)**: pp.445-452.

Arnold, J.G., Potter, K.N., King, K.W. and Allen, P.M., (2005). Estimation of soil cracking and the effect on surface runoff in a Texas Black land Prairie watershed. *Hydrological Processes* ***19*(3)**: pp.589-603.

Baer, J.U., Kent, T.F. and Anderson, S.H., (2009). Image analysis and fractal geometry to characterize soil desiccation cracks. *Geoderma* **154(1)**: pp.153-163.

Berretta, C., Poë, S. and Stovin, V., (2014). Moisture content behaviour in extensive green roofs during dry periods: The influence of vegetation and substrate characteristics. *Journal of Hydrology* **511**: pp.374-386.

Blight, G.E., (2003). The vadose zone soil-water balance and transpiration rates of vegetation. *Geotechnique* **53(1)**: pp.55-64.

Bordoloi, S., Hussain, R., Garg, A., Sreedeep, S. and Zhou, W.H., 2017. Infiltration characteristics of natural fiber reinforced soil. *Transportation Geotechnics*, ***12***, pp.37-44.

Bordoloi, S., Garg, A. and Sreedeep, S., (2016). Potential of Uncultivated, Harmful and Abundant Weed as a Natural Geo-Reinforcement Material. *Advances in Civil Engineering Materials* **5(1)**: pp.276-288.

Bordoloi, S., Yamsani, S.K., Garg, A., Sreedeep, S. and Borah, S., (2015). Study on the efficacy of harmful weed species Eicchornia crassipes for soil reinforcement. *Ecological Engineering* **85**: pp.218-222.

Bordoloi, S., Hussain, R., Garg, A., Sreedeep, S., and Zhou, W. H. (2017a). Infiltration characteristics of natural fiber reinforced soil. Transportation Geotechnics, 12, 37-44.

Bordoloi, S., Kashyap, V., Garg, A., Sreedeep, S., Wei, L., and Andriyas, S. (2017b). Measurement of mechanical characteristics of fiber from a novel invasive weed: A comprehensive comparison with fibers from agricultural crops. Measurement.

Bordoloi, S., Garg, A., and Sreedeep, S., (2017c). A Review of Physio-Biochemical Properties of Natural Fibers and Their Application in Soil Reinforcement," Advances in Civil Engineering Materials, Vol. 6, No. 1, pp. 1–37, https://doi.org/10.1520/ACEM20160076. ISSN 2379-1357

Bordoloi, S., Sen, S., Hussain, R., Garg, A., and Sreedeep, S., (2017d). "Chemically Altered Natural Fiber Impregnated Soil for Improving Subgrade Strength of Pavements," Advances in Civil Engineering Materials https://doi.org/10.1520/ACEM20170042. ISSN 2379-1357

Bouma, J., Dekker, L.W. and Haans, J.C.F.M., (1979). Drainability of some Dutch clay soils: a case study of soil survey interpretation. *Geoderma*, **22(3)**: pp.193-203.

Chaduvula, U., Viswanadham, B.V.S. and Kodikara, J., (2017). A study on desiccation cracking behavior of polyester fiber-reinforced expansive clay. *Applied Clay Science*.

Chertkov, V.Y. and Ravina, I., (1999). Tortuosity of crack networks in swelling clay soils. *Soil Science Society of America Journal* **63(6)**: pp.1523-1530.

Coles, N., Trudgill, S., (1985). The movement of nitrogen fertilizer from the soil surface to drainage waters by preferential flow in weakly structured soils Slapton South Devon UK. *Agriculture, Ecosystems & Environment* **13**: 241–259.

Corte, A. and Higashi, A., (1960). Experimental Research on Desiccation Cracks, *Soil Research report 66: U. S. Army Snow Ice and Permifrost Research Establishment, Willmette, Illinous*.

Costa, S., Kodikara, J. and Shannon, B., (2013). Salient factors controlling desiccation cracking of clay in laboratory experiments *Géotechnique* **63(1)**: 18.

Dasog, G.S., Acton, D.F., Mermut, A.R. and JONG, E.D., (1988). Shrink-swell potential and cracking in clay soils of Saskatchewan. *Canadian Journal of Soil Science* **68(2)**: pp.251-260.

El Abedine, A.Z. and Robinson, G.H., (1971). A study on cracking in some vertisols of the Sudan. *Geoderma* 5(3), pp.229-241.

Fox, W.E., (1964). Cracking characteristics and field capacity in a swelling soil. *Soil Sci* **98(413)**: pp.37-49.

Gadi, V.K., Tang, Y.R., Das, A., Monga, C., Garg, A., Berretta, C. and Sahoo, L., 2017. Spatial and temporal variation of hydraulic conductivity and vegetation growth in green infrastructures using infiltrometer and visual technique. CATENA, **155**, pp.20-29.

Gadi, V.K., Bordoloi, S., Garg, A., Kobayashi, Y. and Sahoo, L., 2016. Improving and correcting unsaturated soil hydraulic properties with plant parameters for agriculture and bioengineered slopes. *Rhizosphere*, ***1***, pp.58-78.

Garg, A., Coo, J.L. and Ng, C.W.W., (2015c). Field study on influence of root characteristics on soil suction distribution in slopes vegetated with Cynodon dactylon and Schefflera heptaphylla. *Earth Surface Processes and Landforms*, ***40*****(12)**, pp.1631-1643.

Garg, A., Leung, A.K. and Ng, C.W.W., (2015a). Transpiration reduction and root distribution functions for a non-crop species Schefflera heptaphylla. *Catena* ***135*****:** pp.78-82.

Garg, A., Leung, A.K. and Ng, C.W.W., (2015b). Comparisons of soil suction induced by evapotranspiration and transpiration of S. heptaphylla. *Canadian Geotechnical Journal* **52(12)**: pp.2149-2155.

Hazra, B., Gadi, V., Garg, A., Ng, C.W.W. and Das, G.K., (2017). Probabilistic analysis of suction in homogeneously vegetated soils. *Catena* **149:** pp.394-401.

Heede, B.H., (1971). Characteristics and processes of soil piping in gullies. *USDA Forest Service Research Paper* **RM-68**: pp. 15.

Hemmati, S., Gatmiri, B., Cui, Y.J. and Vincent, M., (2012). Thermo-hydro-mechanical modelling of soil settlements induced by soil-vegetation-atmosphere interactions. *Engineering Geology* **139**: pp.1-16.

Jayanthi, P.N.V., Kuntikana, G. and Singh, D.N., (2017). Stabilization of Fine-Grained Soils Against Desiccation Cracking Using Sustainable Materials. *Advances in Civil Engineering Materials* **6(1)**: pp.36-67.

Johnston, J.R. and Hill, H.O., (1944). A study of the shrinking and swelling properties of rendzina soils. *Soil Science Society of America Journal* **9(C)**: pp.24-29.

Leung, A.K., Garg, A. and Ng, C.W.W., (2015b). Effects of plant roots on soil-water retention and induced suction in vegetated soil. *Engineering Geology* **193:** pp.183-197.

Leung, A.K., Garg, A., Coo, J.L., Ng, C.W.W. and Hau, B.C.H., (2015a). Effects of the roots of Cynodon dactylon and Schefflera heptaphylla on water infiltration rate and soil hydraulic conductivity. *Hydrological processes* **29(15)**: pp.3342-3354.

Li, J.H. and Zhang, L.M., (2010). Geometric parameters and REV of a crack network in soil. *Computers and Geotechnics* **37(4)**: 466-475.

Li, J.H. and Zhang, L.M., (2011). Study of desiccation crack initiation and development at ground surface. *Engineering Geology* **123(4)**: pp.347-358.

Li, J.H., Li, L., Chen, R. and Li, D.Q., (2016). Cracking and vertical preferential flow through landfill clay liners. *Engineering Geology* **206**: pp.33-41.

Logsdon, S., Allmaras, R.R., Wu, L., Swan, J.B. and Randall, G.W., (1990). Macroporosity and its relation to saturated hydraulic conductivity under different tillage practices. *Soil Science Society of America Journa*l, **54(4)**: pp.1096-1101.

Macai-Pasqualino, E.J., Costes, N.C. and Parker, J.K., (1993). Digital image techniques for volume change measurements in triaxial tests. In *Digital Image Processing: Techniques* *and Applications in Civil EngineeringAmerican Society of Civil EngineersNational Science FoundationEngineering Foundation*.

Mi, H., (1995). Kinematic wave formulation for flow through macroporous soil. Ph.D. Thesis, Department of Civil and Environmental Engineering, Wayne State University, Detroit, MI.

Miller, C.J., Mi, H. and Yesiller, N., (1998). Experimental analysis of desiccation crack propagation in clay liners. *JAWRA Journal of the American Water Resources Association*, ***34*****(3)**: pp.677-686.

Mitchell, A.R. and Van Genuchten, M.T., (1992). Shrinkage of bare and cultivated soil. *Soil Science Society of America Journal* **56(4)**: pp.1036-1042.

Ollobarren, P., Capra, A., Gelsomino, A. and La Spada, C., (2016). Effects of ephemeral gully erosion on soil degradation in a cultivated area in Sicily (Italy). *CATENA* **145**: pp.334-345.

Rasband, W.S., (2011). ImageJ. US National Institutes of Health, Bethesda, 616 Maryland, USA.

Rayhani, M.H.T., Yanful, E.K. and Fakher, A., (2008). Physical modeling of desiccation cracking in plastic soils. *Engineering Geology* **97(1)**: pp.25-31.

Ringrose-Voase, A.J. and Sanidad, W.B., (1996). A method for measuring the development of surface cracks in soils: application to crack development after lowland rice. *Geoderma* **71(3)**: pp.245-261.

Schneider, C.A., Rasband, W.S. and Eliceiri, K.W., (2012). NIH Image to ImageJ: 25 years of image analysis. *Nat methods* **9(7)**: pp.671-675.

Singh, B.B., Ajeigbe, H.A., Tarawali, S.A., Fernandez-Rivera, S. and Abubakar, M., (2003). Improving the production and utilization of cowpea as food and fodder. *Field Crops Research* **84(1)**, pp.169-177.

Snow, D.T., (1969). Anisotropie permeability of fractured media. *Water Resources Research* **5(6):** pp.1273-1289.

Solleti, S.K., Bakshi, S., Purkayastha, J., Panda, S.K. and Sahoo, L., (2008). Transgenic cowpea (Vigna unguiculata) seeds expressing a bean α-amylase inhibitor 1 confer resistance to storage pests, bruchid beetles. *Plant cell reports* **27(12)**: pp.1841-1850.

Stovin, V., Poë, S. and Berretta, C., 2013. A modelling study of long term green roof retention performance. *Journal of environmental management* **131**: pp.206-215.

Swartz, G.L., (1966). Water entry into a black earth under flooding. Queensl. *J. Agric. Anim. Sci* **23**: pp.407-422.

Tang, C.S., Shi, B., Cui, Y.J., Liu, C. and Gu, K., (2012). Desiccation cracking behavior of polypropylene fiber–reinforced clayey soil. *Canadian Geotechnical Journal* **49(9)**: pp.1088-1101.

Thomas, G.W. and Phillips, R.E., (1979). Consequences of water movement in macropores. *Journal of Environmental Quality* **8(2)**: pp.149-152.

Torres, M.A., Armenteros, E.D.L., Fernández, R.O. and Fernández, P.G., (2004). Digital image analysis for the estimation of cracked areas and the soil shrinkage characteristic curve in clay soils amended with composted sewage sludge. *Spanish Journal of Agricultural Research* **2(3)**: pp.473-479.

Vardhan, H., Bordoloi, S., Garg, A. and Garg, A., (2017). Compressive strength analysis of soil reinforced with fiber extracted from water hyacinth. *Engineering Computations* **34(2)**.

Wang, C., Zhang, Z.Y., Liu, Y. and Fan, S.M., (2017). Geometric and fractal analysis of dynamic cracking patterns subjected to wetting-drying cycles. *Soil and Tillage Research* **170**: pp.1-13.

Waugh, W.J., Thiede, M.E., Bates, D.J., Cadwell, L.L., Gee, G.W. and Kemp, C.J., (1994). Plant cover and water balance in gravel admixtures at an arid waste-burial site. *Journal of Environmental Quality* **23(4)**: pp.676-685.

Yesiller, N., Miller, C.J., Inci, G. and Yaldo, K., (2000). Desiccation and cracking behavior of three compacted landfill liner soils. *Engineering Geology* **57(1)**: pp.105-121.

Yoshida, S. and Adachi, K., (2004). Numerical analysis of crack generation in saturated deformable soil under row-planted vegetation. *Geoderma* **120(1)**: pp.63-74.

Young, R., Warkentin, B.P, (2012). Soil properties and behaviour (Vol. 5). Elsevier.

Yuen, K., Graham, J. and Janzen, P., (1998). Weathering-induced fissuring and hydraulic conductivity in a natural plastic clay. *Canadian Geotechnical Journa*l **35(6)**: pp.1101-1108.

Table 1 Engineering properties of soil

Sl. No	Soil property	Value
1	Specific gravity	2.55
2	Grain Size Distribution	
	Coarse Sand (4.75mm-2mm)	0 (%)
	Medium Sand (2mm-0.425mm)	6 (%)
	Fine Sand (0.425mm-0.075mm)	19 (%)
	Silt (0.075mm-0.002mm)	50 (%)
	Clay (<0.002mm)	25 (%)
3	Consistency Limits	
	Liquid Limit	41 (%)
	Plastic Limit	25 (%)
	Shrinkage Index	12 (%)
	Plasticity Index	16 (%)
4	Compaction Characteristics	
	Optimum Moisture Content	17 (%)
	Maximum Dry Density	1.70 (g/cc)

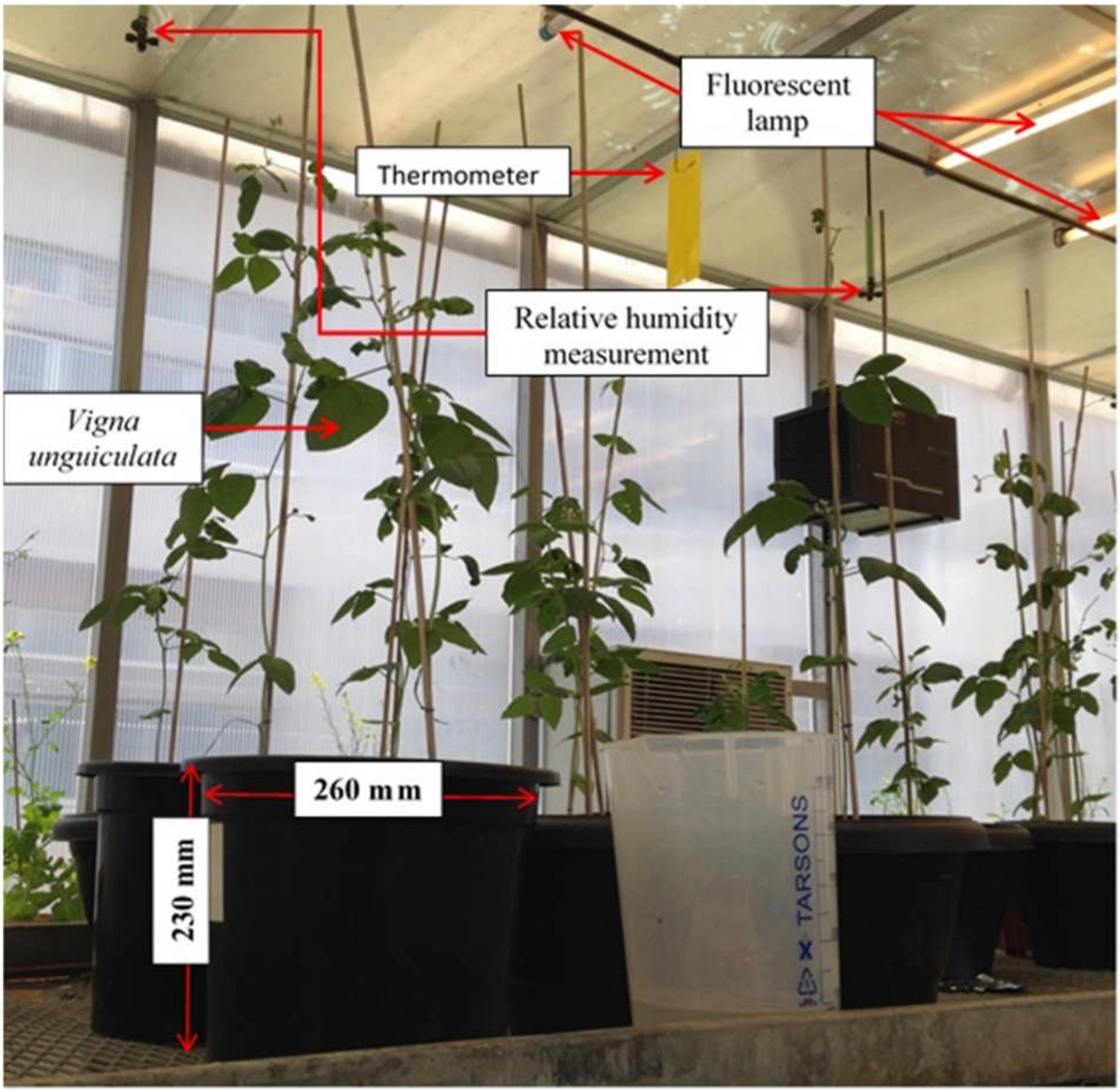

Fig. 1 Overview of experimental setup placed in greenhouse.

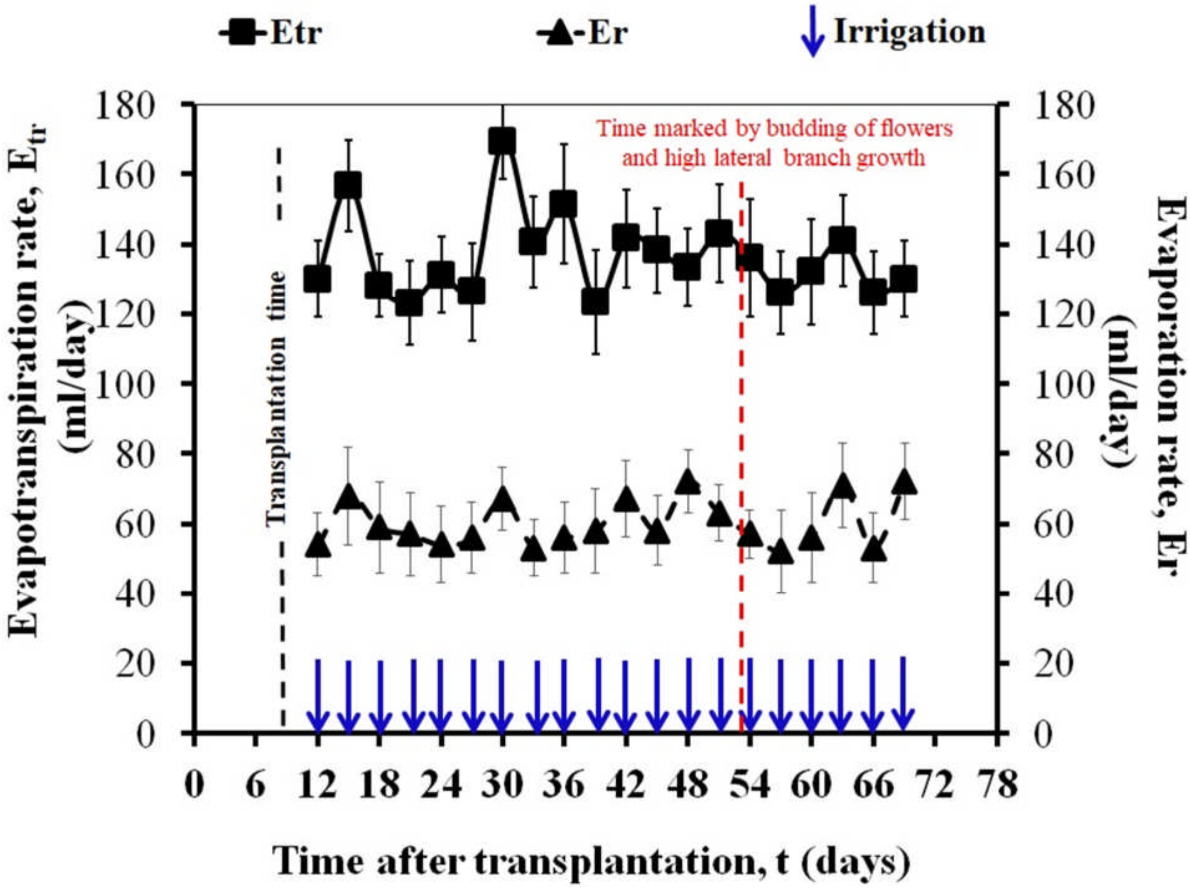

Fig.2 Measured evapotranspiration and evaporation rate of soil along with irrigation schedule during testing period.

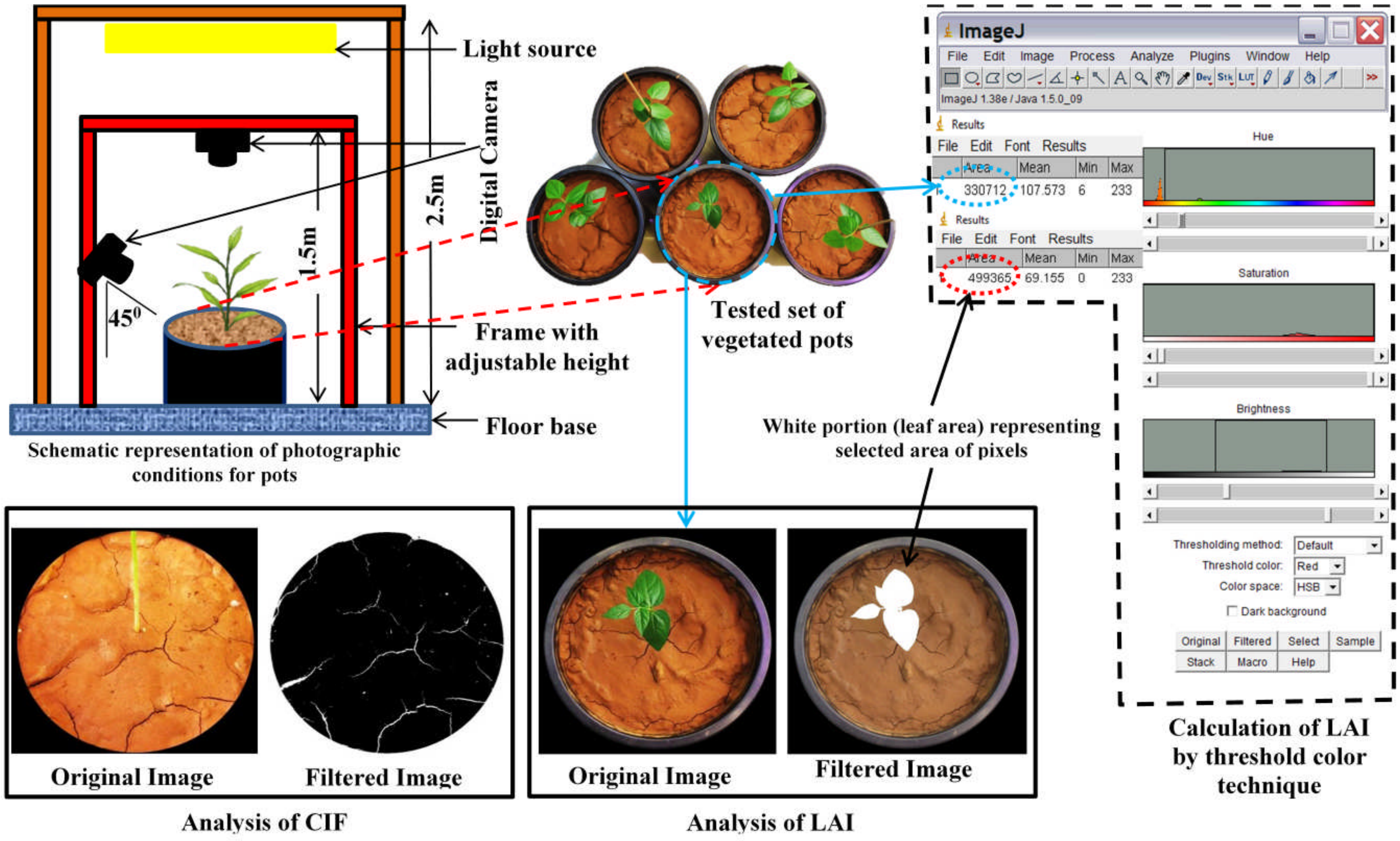

Fig.3 Determination of LAI and CIF respectively by image analysis using threshold color technique.

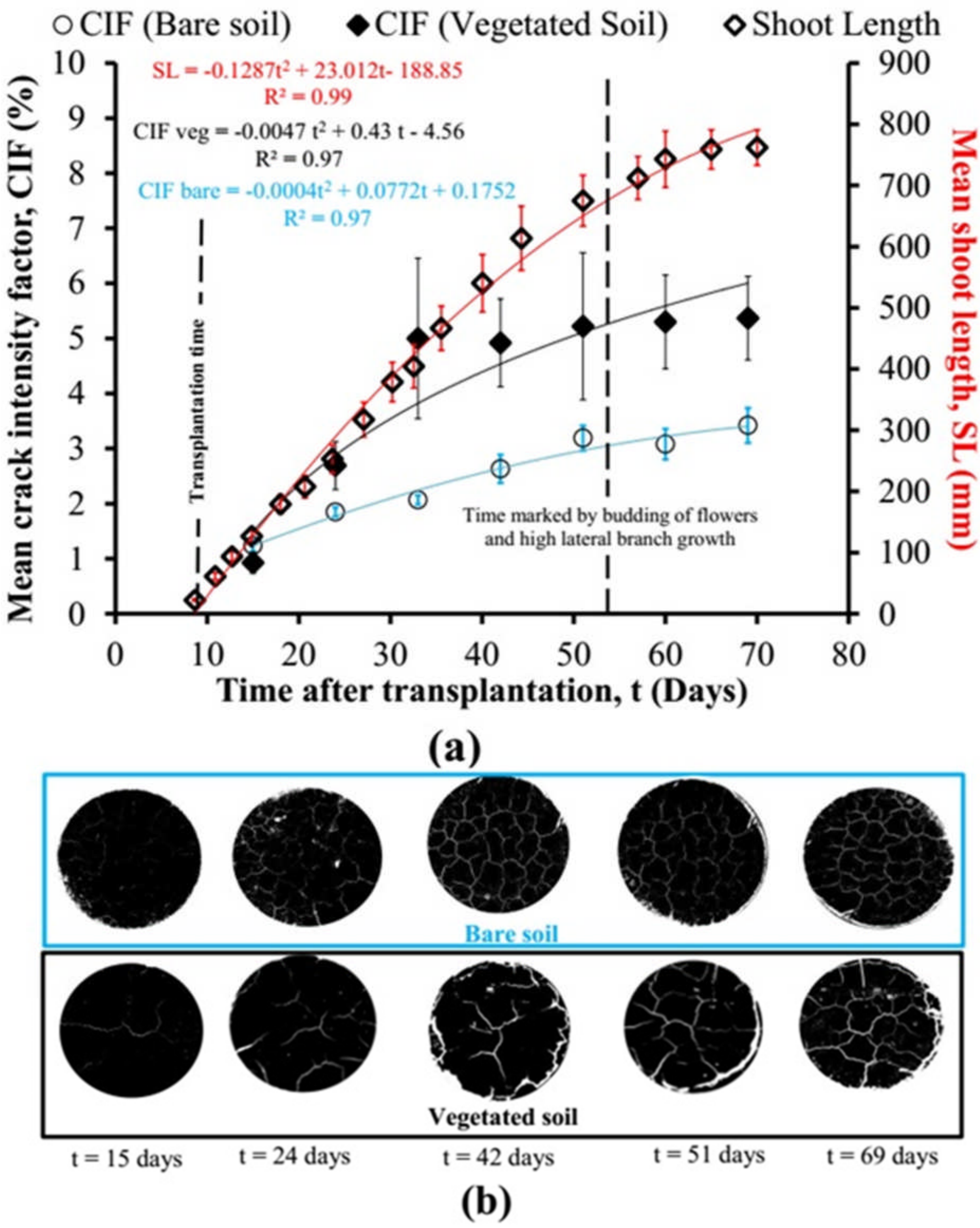

Fig.4 Variation of (a) CIF (bare and vegetated soil) and SL of plant with time (b) Binary image representation of cracks (white section) with time for a single pot (bare and vegetated soil).

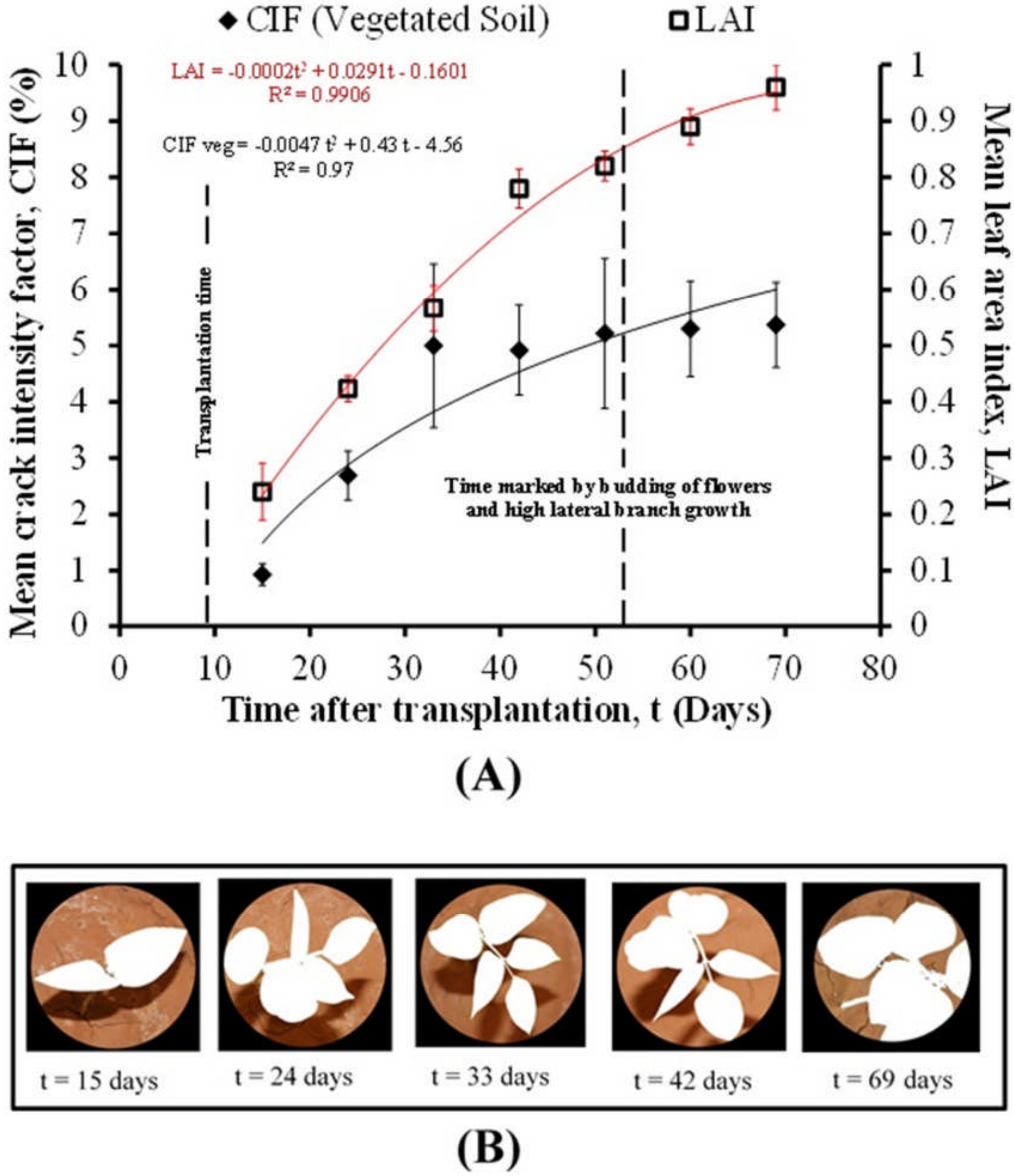

Fig.5 Variation of (a) CIF (vegetated soil) and its corresponding LAI with time (b) threshold image representation of leaf area (white portion) with time for a single pot.